

ACRIM3 and the Total Solar Irradiance database

Richard C. Willson

Received: 16 December 2013 / Accepted: 14 February 2014
© The Author(s) 2014. This article is published with open access at Springerlink.com

Abstract The effects of scattering and diffraction on the observations of the ACRIMSAT/ACRIM3 satellite TSI monitoring mission have been characterized by the preflight calibration approach for satellite total solar irradiance (TSI) sensors implemented at the LASP/TRF (Laboratory for Atmospheric and Space Physics/Total Solar Irradiance Radiometer Facility). The TRF also calibrates the SI (International System of units) traceability to the NIST (National Institute of Standards and Technology) cryo-radiometric scale. ACRIM3's self-calibration agrees with NIST to within the uncertainty of the test procedure (~ 500 ppm). A correction of ~ 5000 ppm was found for scattering and diffraction that has significantly reduced the scale difference between the results of the ACRIMSAT/ACRIM3 and SORCE/TIM satellite experiments. Algorithm updates reflecting more than 10 years of mission experience have been made that further improve the ACRIM3 results by eliminating some thermally driven signal and increasing the signal to noise ratio. The result of these changes is a more precise and detailed picture of TSI variability. Comparison of the results from the ACRIM3, SORCE/TIM and SOHO/VIRGO satellite experiments demonstrate the near identical detection of TSI variability on all sub-annual temporal and amplitude scales during the TIM mission. The largest occurs at the rotational period of the primary solar activity longitudes. On the decadal timescale, while ACRIM3 and VIRGO results exhibit close agreement throughout, TIM exhibits a consistent 500 ppm upward trend relative to ACRIM3 and VIRGO. A solar magnetic activity area proxy for TSI has been used to demonstrate that the ACRIM TSI composite

and its $+0.037$ %/decade TSI trend during solar cycles 21–23 is the most likely correct representation of the extant satellite TSI database. The occurrence of this trend during the last decades of the 20th century supports a more robust contribution of TSI variation to detected global temperature increase during this period than predicted by current climate models.

Keywords Total Solar Irradiance · SI Calibration · Decadal Trends

1 Introduction

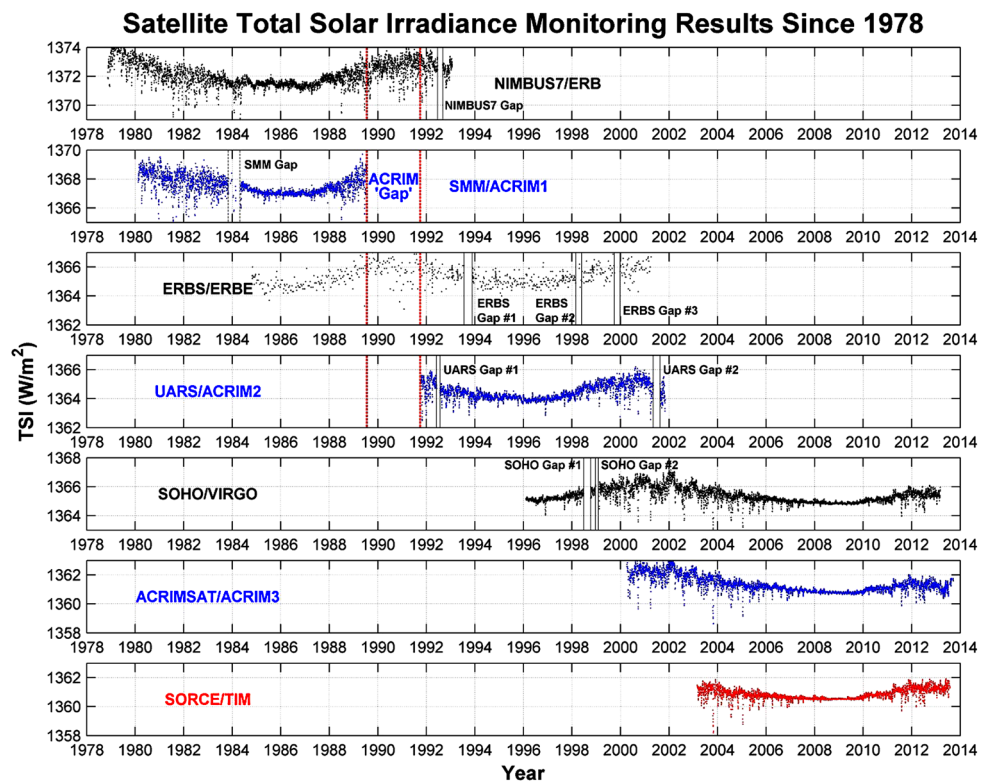
The Earth's climate regime is determined by the total solar irradiance (TSI) and its interactions with the Earth's atmosphere, oceans and landmasses. Evidence from 35 years of satellite TSI monitoring and solar activity data has established a paradigm of direct relationship between TSI and solar magnetic activity. (Willson et al. 1981; Willson and Hudson 1991; Willson 1997, 1984; Frohlich and Lean 1998; Scafetta and Willson 2009; Kopp and Lean 2011a, 2011b) This paradigm, together with the satellite record of TSI and proxies of historical climate and solar variability, support the connection between variations of TSI and the Earth's climate. Recent developments in preflight calibrations of TSI satellite monitors can provide significant improvements in accuracy and traceability of the database and our understanding of solar variability and its importance as a forcing of climate change.

The ACRIMSAT/ACRIM3 and SORCE/TIM flight instruments were characterized in the LASP/TRF by instrument proxies¹ after their launches (Kopp et al. 2012). The

R.C. Willson (✉)
ACRIM, 12 Bahama Bend, Coronado, CA 92118, USA
e-mail: acrim@acrim.com

¹ACRIM3 and TIM backup instruments were tested and assumed to represent the flight versions.

Fig. 1 Satellite TSI experiment results contributing to the TSI database. The inclusion of pre-1992 results in a TSI composite time series requires ‘bridging the ACRIM Gap’ with either the Nimbus7/ERB or ERBS/ERBE results. The choices produce significantly different decadal trending in the resulting TSI composite



principal finding for ACRIM3 was that instrumental scattering and diffraction has a significant effect on its results. After reprocessing data to conform its results to this TRF test result the ACRIM3 TSI values agree more closely with those of TIM. Other TSI flight instrumentation, including proxies for the SOHO/VIRGO and SOHO/DIARAD (Frohlich et al. 1997) experiments as well as the PICARD/PREMOS flight instrument (Schmutz et al. 2013), have been characterized at the TRF. Application of the characterizations have resulted in flight observations in closer agreement with TIM TSI values as was found with ACRIM3. Preflight calibrations such as those made at the LASP/TRF can normalize TSI satellite monitoring experiments with greater precision than sensor self-calibrations and improve the long term traceability of the TSI database.

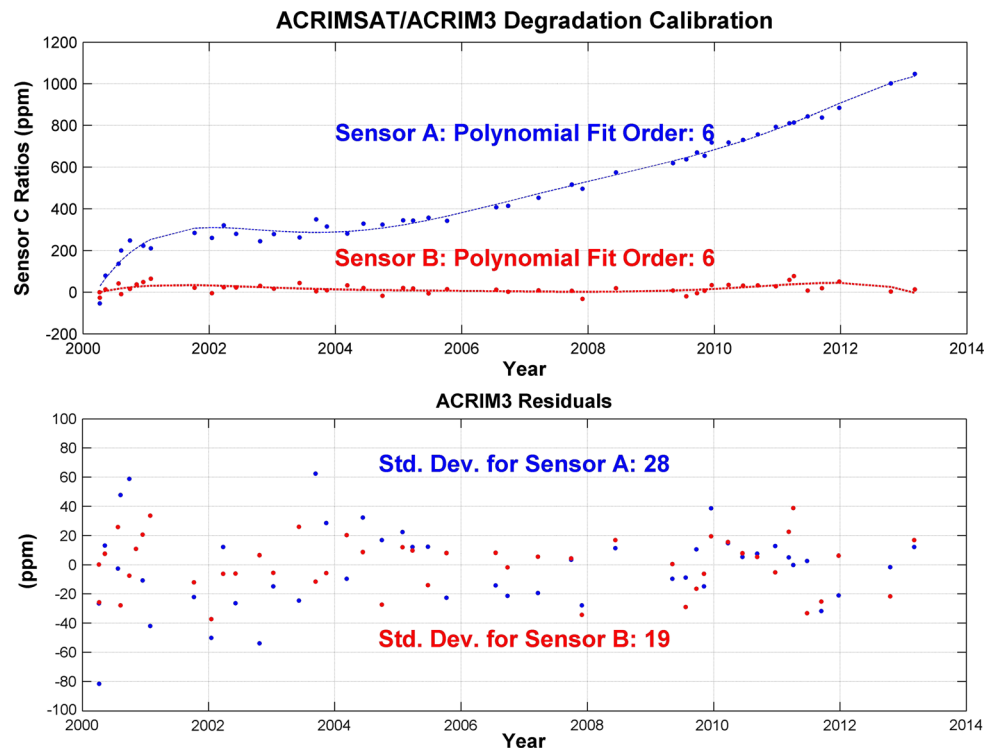
One of the most perplexing issues in the 35 year satellite TSI database is the disagreement among TSI composite time series in decadal trending. Two such constructions frequently cited are the ACRIM and PMOD composites. A hiatus of dedicated, precision TSI monitoring was caused by the termination of the SMM/ACRIM1 experiment in mid-1989 and the delay in launching UARS/ACRIM2 until late 1991. During the resulting ‘ACRIM Gap’ two Earth radiation budget experiments, the Nimbus7/ERB and ERBS/ERBE, provided TSI results. The ERB and ERBE results lacked the accuracy, precision, measurement cadence and on-orbit degradation self-calibration of dedicated TSI monitors. Additionally, the choice of ERB or ERBS results to bridge

the ACRIM Gap through comparisons with ACRIM1 and ACRIM2 give significantly different results for TSI decadal trending. The ACRIM and PMOD TSI composite time series use the ERB and ERBE results, respectively, to bridge the Gap. Decadal trending during solar cycles 21–23 is significant for the ACRIM composite but not for the PMOD. A new TSI-specific TSI proxy database has been compiled that appears to resolve the issue in favor of the ACRIM composite and trend. The resolution of this issue is important for application of the TSI database in research of climate change and solar physics.

1.1 The satellite TSI database

The suite of extant TSI monitoring results is shown in Fig. 1. The first satellite TSI experiment was the NOAA Nimbus 7/Earth Radiation Budget (Nimbus7/ERB), an experiment designed to provide data for earth radiation budget (ERB) studies (Hickey et al. 1988; Hoyt et al. 1992). This was followed by the Solar Maximum Mission/Active Cavity Radiometer Irradiance Monitor 1 (SMM/ACRIM1: 1980–1989), the first experiment specifically designed to monitor TSI for the long term climate database and capable of self-calibrating the on-orbit degradation of its sensors (Willson et al. 1981). Next was the NOAA Earth Radiation Budget Satellite/Earth Radiation Budget Experiment (ERBS/ERBE: 1984–2003) that used a mission-adapted version of the ACRIM2 sensor design (Lee et al. 1995).

Fig. 2 ACRIM3 mission sensor degradation self-calibration results. The plot shows the ratios of C/A and C/B plotted relative to their initial as-launched values in units of parts per million (ppm). The shutter of sensor A operates continuously while the shutters of sensors B and C are operated briefly every 90 days. The C/A ratio calibrates sensor A solar exposure degradation and the C/B ratio facilitates calibration of non-solar exposure degradation



The Upper Atmospheric Research Satellite/Active Cavity Radiometer Irradiance Monitor 2 (UARS/ACRIM2: 1991–2001) (Willson 1997) was intended to overlap SMM/ACRIM1 but the Challenger disaster delayed its shuttle-based launch for two years. The resulting ‘ACRIM Gap’ has provided one of the major controversies in constructing a composite TSI time series. This is because the ERB and ERBE experiments produce significantly different results when used to bridge the Gap through overlapping comparisons with ACRIM1 and ACRIM2 (see Sect. 3 below).

The Solar and Heliospheric Observatory/Variability of solar IRradiance and Gravity Oscillations experiment (SOHO/VIRGO: 1996→) was the first of four currently ongoing TSI experiments to be deployed (Frohlich et al. 1997). The second was the ACRIM SAT/Active Cavity Radiometer Irradiance Monitor 3 experiment (ACRIMSAT/ACRIM3: 2000→) (Willson 2001; Willson and Mordvinov 2003). The third was the Solar Radiation and Climate Experiment/Total Irradiance Monitor experiment (SORCE/TIM: 2003→) (Kopp et al. 2005a, 2005b). The fourth is the Total Solar Irradiance Calibration Transfer Experiment (TCTE) launched in late 2013 on the US Air Force Space Test Program spacecraft known as STPSat-3.

1.2 Self-calibrating TSI sensors

The sensors used to make satellite observations of TSI thus far are electrically self-calibrated cavity pyrheliometers. These thermal detectors compare the heating of their

sensors by TSI with that of electrical power in a shuttered, differential mode. Interpretation of measurements in the international system of units (SI) is accomplished through electrical power calibrations and metrology of the sensor’s physical properties including its aperture area and efficiency for absorbing TSI (Willson 1979, 1999). TSI results are reported on the ‘native scales’ of their sensors in SI units defined by the above self-calibrations and modeled diffraction and scattering. This type of calibration is frequently referred to as ‘self-calibrated’ or ‘component calibration’.

The precision of TSI monitors is orders of magnitude less uncertain than their accuracies in SI units so comparison of the overlapping results of a series of satellite monitors can provide the maximum possible traceability for composite TSI time series. The uncertainty of ACRIM3 degradation self-calibration on orbit is less than $5 \text{ ppm}^2/\text{year}$, for example (as seen in Fig. 2), while its ‘self-calibrated’ SI uncertainty or accuracy is $\sim \pm 500 \text{ ppm}$ (see Fig. 3).

1.3 Cryogenic radiometry

Radiometers operating at the temperature of liquid Helium (LHe) have significantly reduced sources of thermally driven measurement uncertainties and can make TSI scale observations with high SI traceability. Early development of this technology at the UK National Physical Laboratory

²ppm: parts per million.

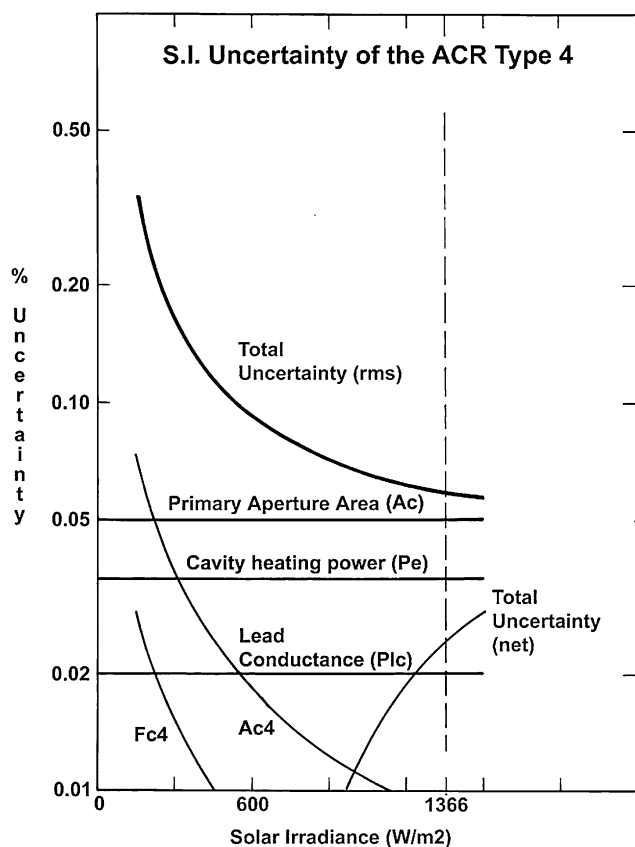


Fig. 3 Uncertainties of modeled ACRIM3 self-calibration (SI units) derived from parametric analysis of sensor components, optical and electrical properties (Willson 1999, Algorithm Theoretical Basis Document)

(NPL) (Martin et al. 1985) was followed by a LHe cryoradiometer calibration facility developed by the US National Institute of Standards and Technology (NIST) (Datla et al. 1992; Houston and Rice 2006). Application of the NIST technology to the investigation of satellite TSI radiometer calibrations was studied by Butler et al. (2008).

More recently the Total Solar Irradiance Radiometer Facility (TRF) using a LHe cryo-radiometer and laser transfer system was developed at the Laboratory for Astronomy and Space Physics (LASP) to calibrate the GLORY/TIM TSI instrumentation (GLORY/TIM launch failed in 2011) (Kopp and Lean 2013).

The LASP/TRF was specifically designed for the calibration and characterization of TSI satellite sensors. SI scale realizations are traceable to NIST. While the SI uncertainty of TSI sensor self-calibrations is not less than ± 500 ppm at the TSI level, cryo-radiometer calibrations can theoretically approach a few hundreds of ppm (Kopp et al. 2012). In addition the TRF has the ability to calibrate the effects of scattering and diffraction on TSI sensors' results. This is important because scattering and diffraction effects can be large compared to the SI scale uncertainty and vary with the specific design of each satellite instrument.

The TRF has been used to calibrate scale, scattering and diffraction effects for most of the current generation of satellite TSI instrumentation. Results have been published for TRF tests of the ACRIM3 flight backup instrument (Kopp et al. 2012), the PICARD/PREMOS (Schmutz et al. 2013) and PICARD/SOVAP (Meftah et al. 2013) sensors and the SOHO/VIRGO/PMO6 (Frohlich 2013) and SOHO/VIRGO/DIARAD (Meftah et al. 2013) TSI instrumentation.

1.4 Satellite TSI instrumentation

The extant TSI database contains results from two distinct classes of TSI experiment. The first is the high accuracy, self-calibrating TSI monitors with rapid observational cadence (\sim minutes), precise solar pointing and sensor degradation calibration capability. These are specifically designed to meet the requirements of a climate TSI database with high multi-decadal traceability. All satellite TSI monitoring experiments to date, except the ERB, ERBE and TCTE experiments, have been of this type. The TCTE instrument is capable of operating as a high accuracy, self-calibrating TSI monitor but observes from a non-solar pointing satellite that is re-orientated to provide it with a view of the sun at least once per week. The quality of its results will depend on the solar pointing precision and instrument response to thermal transients caused by satellite re-orientation.

The earth radiation budget experiments are the second class of TSI satellite experiment. They were designed for a scientific investigation that requires less traceability, accuracy and observational cadence. The traceability of ERB and ERBE results are degraded, relative to the TSI monitors, by: (1) the absence of dedicated solar pointing, (2) brief and infrequent data acquisition opportunities; (3) inability to calibrate sensor degradation and (4) infrequent electrical self-calibration. Both ERB and ERBE are on nadir-staring satellites that provide solar views only briefly during an orbit. Nimbus7/ERB obtained solar observation three days out of four during most of its mission. ERBE observation opportunities were less frequent, lasting about 5 minutes and occurring every two weeks. Lacking solar pointing, data were acquired by both ERB and ERBE experiments while the sun passed through their fields of view. This further increases the uncertainty of their observations due to the non-uniform sensitivity of these types of sensors with view angle. Precision and accuracy was also degraded for both ERB and ERBE because of electrical self-calibrating only every two weeks instead of before and after every solar observation as with the TSI monitors.

1.5 ACRIM instrumentation

The development of ACRIM TSI instrumentation began in the 1960's with physical modeling of self-calibrating, cav-

ity pyrheliometric sensor technology. Early ACRIM instruments were deployed in high altitude balloon and sounding rocket experiments to measure TSI (Willson 1967, 1971, 1973, 1978). The models indicated a theoretical lower limit for the SI uncertainty of ACRIM sensors of about ± 500 ppm at TSI levels (see in Fig. 3) (Willson 1979).

A series of ACRIM TSI satellite monitoring experiments began in 1980 with ACRIM1. This was followed by ACRIM2 in 1991 and continues at present with ACRIM3 (launched in 1999). ACRIM experiments on satellites have provided accurate and precise results during more than 90 % of the existing 35 years of the satellite TSI database. High altitude balloon, sounding rocket and space shuttle ACRIM experiments have been conducted since 1976 as under-flight comparisons with satellite experiments (Willson 1973, 1978, 1984).

The native scale of ACRIM1 results is significantly higher than ACRIM2 or 3, as can be seen in Fig. 1. ACRIM2 results were close to the original native scale of ACRIM3 which was ~ 0.3 % higher than the SORCE/TIM results. Investigation of the scale differences between results of the various satellite TSI experiments to improve the precision, accuracy and long term traceability of the composite TSI database is an important focus of current research.

2 TRF recalibration of ACRIM3 results

Investigation of the scale difference between ACRIM3 and TIM results has been conducted by testing the ACRIM3 flight backup instrument at the LASP/TRF (Kopp et al. 2012). The backup was fabricated at the same time as the ACRIM3 flight instrument providing a high probability that its test responses would be representative of the ACRIM3 flight instrumentation.

The TRF calibrates a high powered laser in SI units using a self-calibrating cryogenic radiometer, similar in design to the self-calibrating ambient temperature sensors employed by satellite TSI monitors, but operated at liquid Helium (LHe) temperature. The scale defined at the TRF is traceable to SI units through the NIST cryo-radiometer scale. The calibrated laser is then used as a transfer standard to irradiate ‘ambient temperature’ satellite sensors, comparing their basic ‘self-calibrated’ SI scale to that defined by the calibrating LHe detector. At LHe temperatures self-calibrating irradiance sensors can define TSI level with theoretical SI uncertainties approaching a few hundred parts per million (ppm). The beam size and shape of the TRF laser can be varied to elucidate the effects of scattering and diffraction on sensor results as well.

2.1 ACRIM3 results and degradation self-calibration

Results from the primary radiometer sensor (A) used for full time TSI monitoring is compared with data from the

two identical reference sensors (B and C) every 90 days to calibrate degradation. The backup sensors, because of their limited exposure to solar shortwave radiation, are assumed to experience negligible solar exposure related degradation compared to the primary sensor. The relative performance of the backup sensors provides a non-solar exposure uncertainty limit for the degradation calibration of the primary sensor.

Total degradation of the ACRIM3 primary monitoring sensor has been 900 ppm during the 13 1/2 years of the mission. A degradation profile for the primary sensor is derived from the multi-sensor comparisons and applied as a correction to the results. The standard deviation of the residuals for the degradation profile of the primary sensor is 29 ppm over the mission (see Fig. 2).

Total degradation of the ACRIM3 secondary degradation calibration sensor (B) has been <30 ppm during the mission. The standard deviation of the residuals for the degradation profile of the secondary sensor is 18 ppm, vindicating the assumption that degradation of the reference sensors has not been sufficient to significantly affect the degradation calibration of the primary sensor.

2.2 ACRIM3 TRF characterizations of scattering, diffraction and basic scale

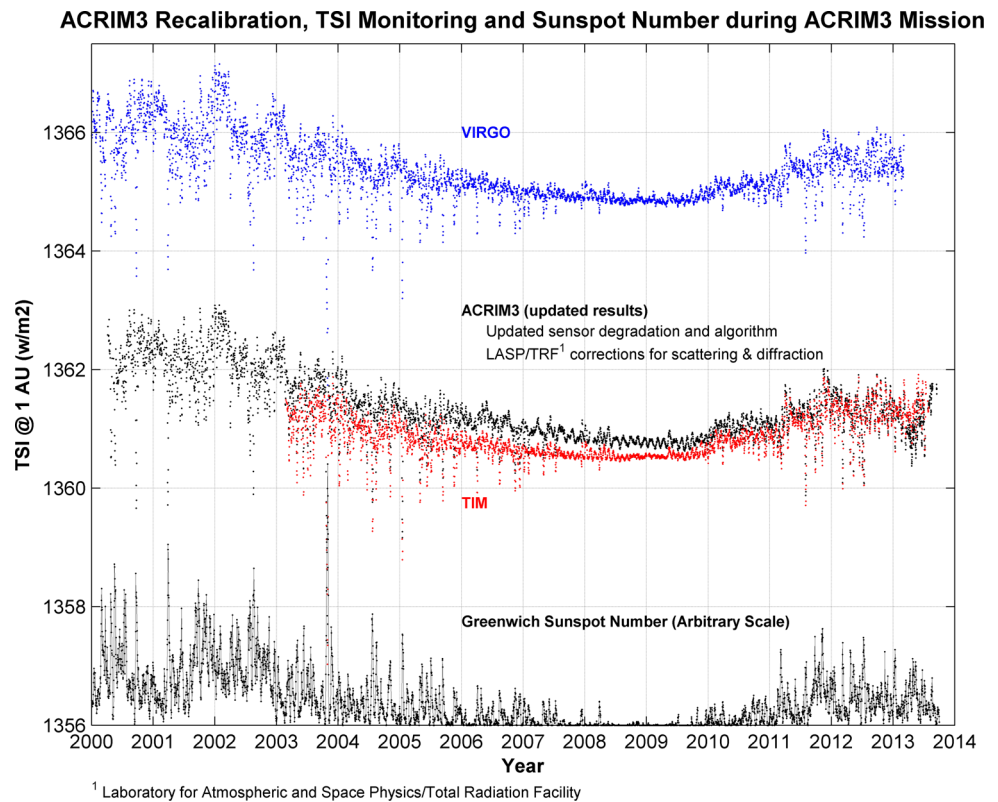
The scattering, diffraction and basic scale properties of the ACRIM3 flight backup instrument were characterized at the LASP/TRF in a series of tests in late 2010 and early 2011. A net downward correction of 5025 ppm was found to be required to account for instrumental scattering and diffraction to conform ACRIM3 results to the TRF characterization (Willson 2011; Kopp et al. 2012). Personnel from the Naval Research Laboratories (NRL) participated in the 2010–2011 ACRIM3 TRF testing as independent observers and conducted additional testing and analyses of ACRIM3 sensor properties as well (Morrill et al. 2013).

The LASP interpretation of TRF results for scattering, diffraction and basic scale correction factors was found to agree with the ACRIM interpretation to well within their mutual error bounds (Kopp and Lean 2011a, 2011b). A similar result was found by the NRL (Willson 2011; Morrill et al. 2013) (see Table 1).

Table 1 Corrections (in ppm) of ACRIM3 results for scattering and diffraction derived from the LASP/TRF testing by the ACRIM, LASP and NRL teams

TRF Analysis	ACRIM3 Correction (ppm)	Uncertainty (+/–)
ACRIM	–5025	~500
LASP	–5400	~500
NRL	–4100	~500

Fig. 4 ACRIM3, TIM, VIRGO and Greenwich Sunspot Number time series after using TRF-derived corrections and algorithm updates to derive ACRIM3 results



The uncertainty of ACRIM3 TRF results can be decreased by obtaining more comparisons with smaller drift between ACRIM3 and TRF cryogenic radiometer exposures than in the original testing. Additional TRF tests are planned for ACRIM sensors to increase the accuracy of ACRIM3 corrections and provide characterizations for the ACRIM sensors used in the SMM/ACRIM1 and UARS/ACRIM2 experiments as well. Since ACRIM results cover more than 90 % of the extant satellite TSI database, a more accurate knowledge of their scattering, diffraction and basic scale properties will improve the accuracy and traceability of the TSI database from 1978 to the present.

2.3 ACRIM3 algorithm updates

The ACRIM3 data reduction algorithm routines that account for the temperature sensitivity of its analog to digital converter (ADC) electronics were updated during 2013 based on experience during its 13 years of operation. Small, thermally driven, periodic annual TSI variations (~ 300 ppm) were indistinguishable components of the large quasi-annual natural TSI variability during the activity maximum of solar cycle 23 but became visible as a possible instrumental effect during the last solar minimum. The quasi-annual variations, which are synchronized with the 1.09 year frequency of the Earth-Jupiter conjunction cycle (Scafetta and Willson 2013) occur even during solar minima with reduced amplitudes. But a component of them was found to result from

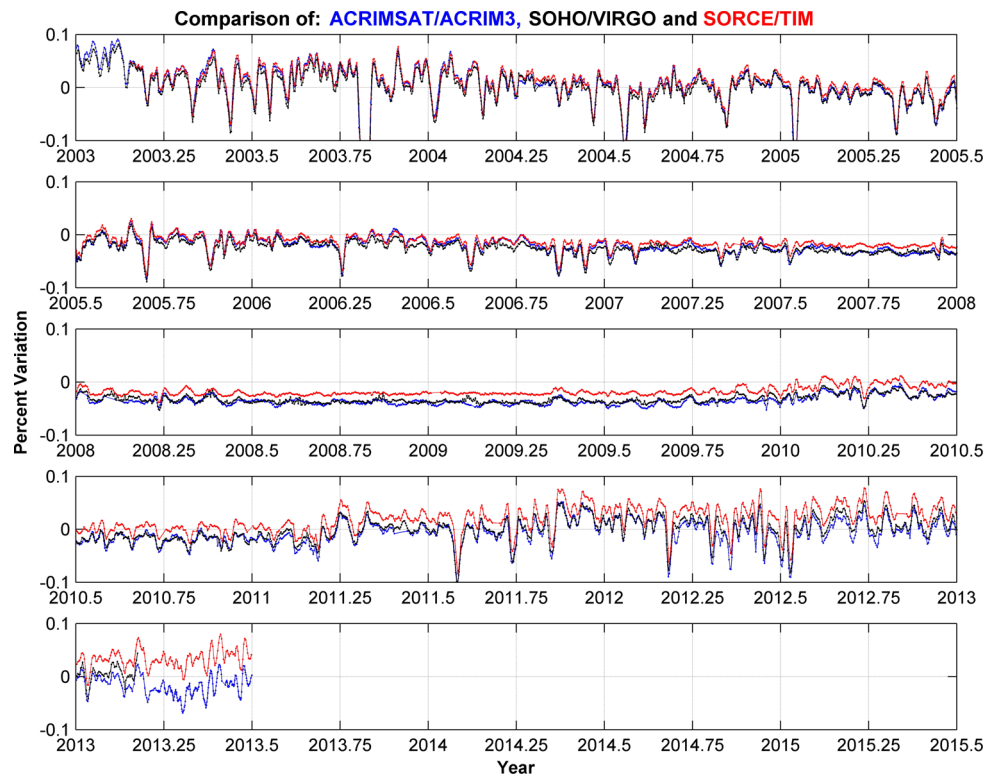
incomplete compensation for the ADC response to changing satellite temperatures caused by the annual eccentricity-driven variation of the Earth's orbit. Another algorithm update refined the parsing of shutter-closed data samples, tying the reference shutter closed electrical calibration phases to the shutter open phase more precisely. The ADC update removed a ~ 300 ppm (peak-to-peak) annual thermal artifact signal from the results. The shutter cycle algorithm update improved the signal to noise ratio of ACRIM3 results.

2.4 Implementation of algorithm updates and application of the TRF corrections

The TRF-derived corrections for scattering and diffraction have been applied to ACRIM3 TSI results by reprocessing the data using the updated algorithms. No correction has been applied for basic SI scale since the agreement between the TRF and ACRIM3 basic SI realizations are within the current error bounds of the TRF testing (~ 500 ppm). As can be seen in Fig. 4, ACRIM3 and TIM results now show much closer agreement in both scale and TSI variability. This is hardly surprising since both were calibrated using the same facility. A remaining issue is what the bounds of uncertainty for the LASP/TRF relative to SI as defined by NIST and how well the instruments reproduce the TRF calibration under flight conditions.

SOHO/VIRGO TSI sensor technology was recently tested at the LASP/TRF and corrections similar those of

Fig. 5 Comparison of TSI variability in ACRIM3, TIM and VIRGO results. The ACRIM3, VIRGO and TIM observations detect most of the same variations most of the time demonstrating their solar origin. The most prominent signal is near the synodic solar rotation rate (~ 27 days) of the solar magnetic activity latitudes (~ 26 deg.). TSI variability is minimal during the extended solar activity minimum period from 2008.7 to 2009.3. TIM exhibits a 500 ppm upward trend during the decade relative to ACRIM3 and VIRGO



ACRIM3 were found that would also put VIRGO results in closer scale agreement with those of SORCE/TIM and the updated ACRIM3. The VIRGO science team has indicated their intent to revise VIRGO results based on the TRF comparison findings (Kopp and Lean 2013).

The TSI variability of the ACRIM3, TIM and VIRGO results are shown in Fig. 5. Of particular interest is the agreement in fine detail of TSI variations in all three records. Most of the small variations, even during the solar minimum period, appear to be periodic. The most visible fall within the range of solar rotational periodicities and are present in all three records. These and many other periodicities that are detected by all three sets of results, are aligned with the harmonics of orbital movements of the planets and the sun relative to the center of mass of the solar system (Scafetta and Willson 2013, 2014).

ACRIM3 and VIRGO detect nearly all the same variations. Most of these are seen by TIM as well except during the least active part of the solar minimum period (2008.7–2009.3) where there is a near absence of variations in the TIM TSI record. VIRGO sees some of the variability detected by ACRIM3 during this time but at lower amplitudes. Lower sensitivities of the VIRGO and TIM sensors may be responsible for these differences.

There is a gradual 500 ppm divergence of TIM results from those of ACRIM3 and VIRGO during the TIM mission, as can be seen in Fig. 5. It is likely due to uncertainties in sensor degradation calibrations and correction.

The close agreement of ACRIM3 and VIRGO results would be compatible with an overcorrection of TIM degradation. This divergence as well as the uncertainty of the degradation calibration capabilities of these instruments will be an important area of investigation in the future because of its importance to the traceability of the long term climate TSI database.

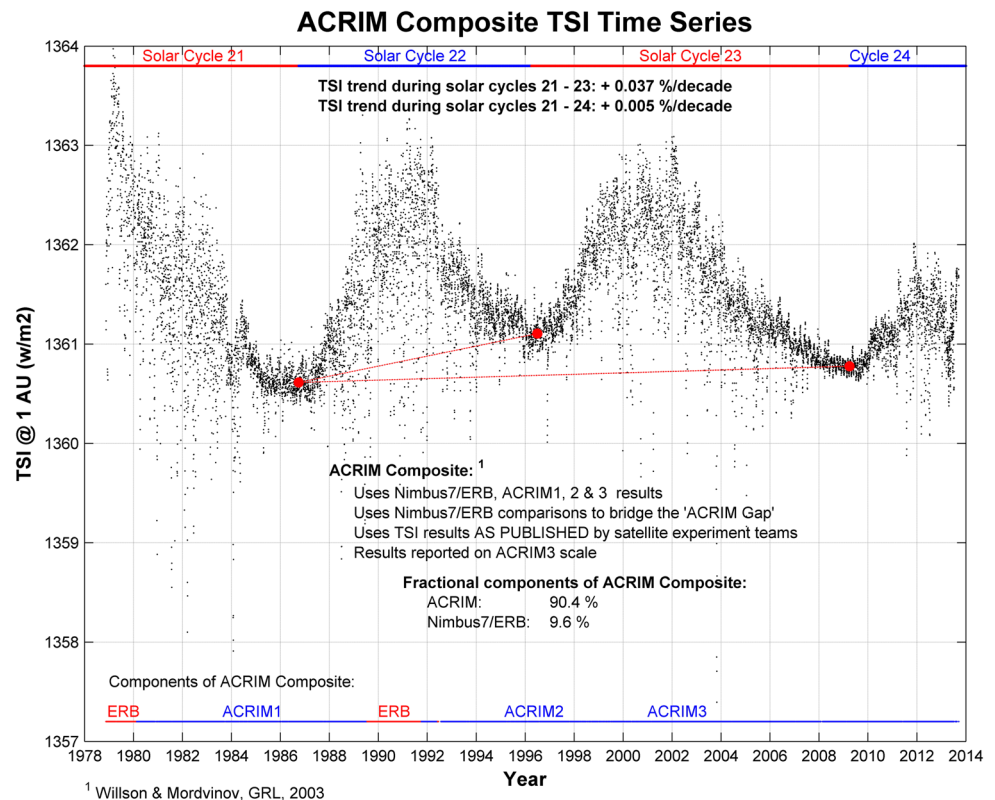
3 The ACRIM composite TSI time series

The most scientifically useful rendering of satellite TSI monitoring experiment results is a composite TSI time series over the more than 35 years of satellite TSI monitoring with useful traceability. A precise composite TSI is an important resource for studies of climate change and solar physics. The series of overlapping satellite results in Fig. 1 provides a contiguous database that can be calibrated relative to any of the experiments through overlapping inter-comparisons over the more than 35 years of observations.

3.1 Updating the ACRIM composite TSI time series

The ACRIM Composite TSI time series (Fig. 6) has been constructed using results from the Nimbus7/ERB, SMM/ACRIM1, UARS/ACRIM2 and ACRIMSAT/ACRIM3 experiments. The ACRIM approach uses original results from each experiment provided by the experiments' science

Fig. 6 The ACRIM composite TSI. Red dots are 6-month means during successive solar minima. The upward trend during solar cycles 21–23 coincides with the sustained rise in the global mean temperature anomaly during the last two decades of the 20th century. The downward trend during solar cycles 23–24 coincides with a cooling trend in the global mean temperature anomaly during the 21st century (UAH GMTA). The tracking of global mean temperature anomaly and TSI is an important result for understanding the relative contribution of solar irradiance and other climate forcings



teams, unmodified by models or assumptions. The philosophy of this approach is that the originally published results best represent the performance of the experiments because the science teams that developed the instrumentation and algorithms that produced their TSI results have the most in-depth knowledge of their experiments. Results are normalized to the updated ACRIM3 results, the best characterized and calibrated of the ACRIM experiments. The ratio of ACRIM1/ACRIM2 results is derived from their comparisons with Nimbus7/ERB.

The most significant feature of the ACRIM Composite TSI for climate change is the +0.037 %/decade trend between the minima separating solar cycles 21–22 and 22–23. This trend over the 9.75 years separating the two minima is significant relative to the ACRIM3 sensor degradation uncertainty (<5 ppm/yr—see Fig. 2). Broad peaks in the ACRIM composite TSI around 1980, 1991 and 2001 correspond to periods of maximum solar magnetic activity during solar cycles 21, 22, and 23. The ~0.1 % variations between magnetic activity maxima and minima, a discovery from the SMM/ACRIM1 experiment, are now well-established features of the sunspot cycle (Willson 1984; Willson et al. 1986). Discovery of the paradigm of direct relationship between solar magnetic activity and TSI (Willson and Hudson 1991) was the key finding that revealed relationships between TSI, historical records of climate and solar magnetic activity (Eddy 1977 and Scafetta and West 2007).

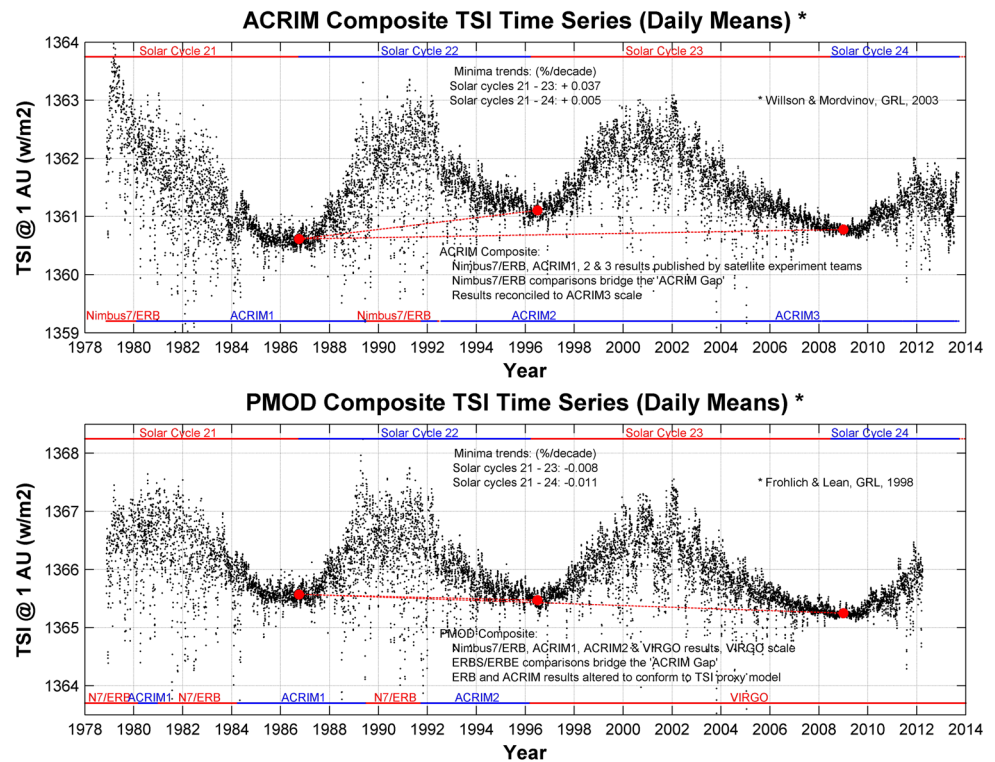
3.2 Comparison of ACRIM and PMOD composites

TSI Composites compiled by the ACRIM (Willson and Mordvinov 2003) and PMOD (Frohlich and Lean 1998, 2004) groups depend on different combinations of TSI observations and assumptions, including the relative scale of their results. The most crucial issue is the database used to 'bridge the ACRIM Gap' for which there are two choices: the Nimbus7/ERB or the ERBS/ERBE. The Nimbus7/ERB choice results in a significant TSI trend during solar cycles 21–22 (seen in the ACRIM composite). The ERBS/ERBE choice results in the lack of a significant trend (seen in the PMOD composite). TSI trends on decadal time scales are consequential for both solar physics and climate change investigations so the choice is an important one.

The ACRIM TSI composite is data driven. It uses ACRIM1, ACRIM2, ACRIM3 and Nimbus7/ERB satellite results published by the experiments' science teams and the highest cadence and quality ACRIM Gap database, the Nimbus7/ERB, to bridge the ACRIM Gap.

The PMOD TSI composite, using results from the Nimbus7/ERB, SMM/ACRIM1, UARS/ACRIM 2 and SOHO/VIRGO experiments, is model driven. It conforms TSI results to a solar-proxy model by modifying published ERB and ACRIM results and choosing the sparse, less precise ERBS/ERBE results as the basis for bridging the ACRIM Gap (Frohlich and Lean 1998).

Fig. 7 Comparison of the ACRIM and PMOD Composite TSI time series. The most significant difference is the ACRIM composite's +0.037 %/decade trend during solar cycles 21–23. Different results near the maxima of solar cycles 21 and 22 are caused by PMOD alteration of some Nimbus7/ERB, ACRIM1 and ACRIM2 results to conform the TSI to the predictions of TSI proxy models



Differences between the two TSI composites are shown in Fig. 7. The most obvious and significant is the solar minimum-to-minimum trend during solar cycles 21–23. ACRIM minima levels show an increase from 1980 to 2000 and a decrease afterward. PMOD shows a continuous decrease since 1978. Other significant differences can be seen during the peak of solar cycles 21 and 22. These arise from ACRIM's use of the original published TSI results from satellite experiment teams while PMOD modifies the results of ERB, ACRIM1 and ACRIM2 to conform them to the predictions of TSI proxy models (Frohlich and Lean 1998).

4 ACRIM composite trend validation

The ACRIM Composite shows a 370 ppm/decade upward trend between the two minima during solar cycles 21–23. The PMOD Composite shows a small negative trend of 80 ppm/decade over this period. The significance of TSI decadal trending for climate change makes the identification of the correct solar cycle 21–22 trend important to establish. To that end a new solar magnetic activity data set, the NSO Kitt Peak Solar Magnetic Flux Strength (Krivova et al. 2007 and Wenzler et al. 2006, 2009) can be used as an independent proxy for TSI during the 'gap'. The SMFS proxy, used to understand the ACRIM Gap and other features of the TSI database in the ACRIM composite, is more specific to TSI than the Mg II and Ca II K chromospheric emission features used as proxies for the PMOD composite model (e.g., Lean

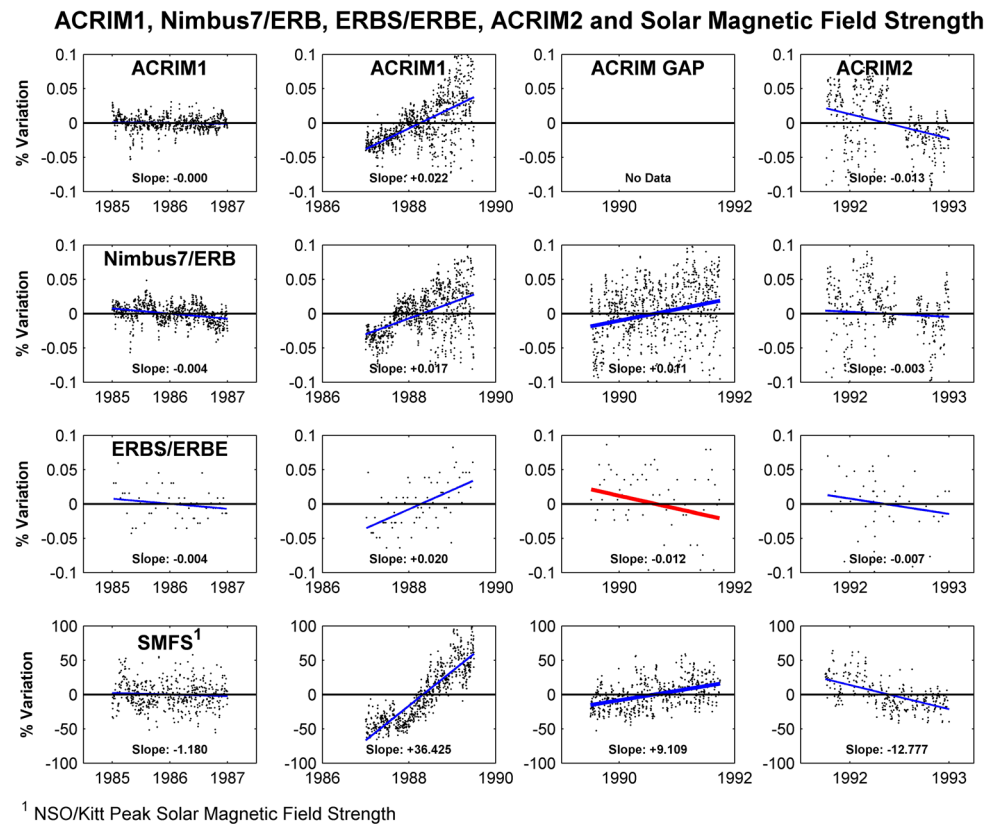
et al. 1995). The SMFS is linked to the dynamics of all solar activity related radiative phenomena while the Mg II and Ca II K proxies are linked to only a subset in the solar chromosphere.

The SMFS 'gap' comparison is shown graphically in Fig. 8. Four time periods are plotted: (1) the solar minimum between solar cycles 21 and 22 (1985–1987), (2) the rising solar activity period up to the start of the ACRIM Gap (1987–1989.5), (3) the ACRIM Gap period (1989.5–1991.75) and (4) the post-gap ACRIM2 comparison period.

The ACRIM1, ERB, ERBE and SMFS trends during the first period agree well and this is not surprising since TSI variation during solar minimum is small. During the increase of solar magnetic activity and TSI variability in the second period, leading up to the maximum of solar cycle 22, general trend agreement of the ACRIM1, ERB, ERBE and SMFS results is also good. The positive slopes and correlation of the TSI and SMFS demonstrate the TSI response expected from the solar magnetic activity-TSI paradigm.

A major difference occurs during the ACRIM Gap where the ERB TSI and the SMFS continue to increase but the ERBE results are anti-correlated, showing a sustained decrease. The most likely cause of ERBE's downward trend is the effect of uncorrected sensor degradation during its first sustained exposure to the enhanced short wavelength fluxes of solar radiation characteristic of periods of maximum solar magnetic activity (Willson et al. 1981). The rate of degradation of TSI sensors is well known to accelerate during periods when a higher component of UV and high energy par-

Fig. 8 Comparison of the ACRIM1, ACRIM1, ERB and ERBE TSI results with the Solar Magnetic Flux strength (SMFS) proxy model TSI results before, during and after the ACRIM Gap. Correlation of the Nimbus7/ERB results with the SMFS during the ACRIM Gap is compatible with the TSI-solar magnetic activity paradigm. Anti-correlation of the ERBS/ERBE during the Gap, incompatible with the paradigm, was likely caused by uncorrected degradation



ticle fluxes are present (Willson 1984). Sensors also tend to eventually reach asymptotes of degradation. The divergence of ERB and ERBE degradation during the ‘gap’ is likely due to the fact that this was the second solar maximum period of exposure for the ERB, which had likely reached its asymptote due to solar maximum exposure during solar cycle 21, and the first time for ERBE, which had not (Willson 1979; Willson and Mordvinov 2003).

The trend difference between the ACRIM and PMOD TSI composites during solar cycles 21–22 is almost exactly equal to the difference between the ERB and ERBE TSI results across the ACRIM Gap. Since the ERB trend conforms to the TSI-solar activity paradigm and the ERBE trend is anti-correlated, the ACRIM TSI composite trend is the most likely correct interpretation of the TSI monitoring database compiled during the 35 years of satellite observations. Another more rigorous approach to analyzing the ACRIM Gap issue using the SMAS came to the same conclusion (Scafetta and Willson 2014).

5 Conclusions

The results of satellite TSI observations were reported on a scale defined by the self-calibration their sensors based on the metrology of their components until recently. This

approach was the only one available to provide high accuracy in the International System of Units (SI). The development of laboratory preflight calibration capabilities, like the LASP/TRF, using cryo-radiometric instrumentation and transfer lasers with sufficient power to simulate TSI irradiance levels now provides greater precision with improved accuracy and the means of characterizing the effects of scattering and diffraction on the measurements of TSI sensors. Scattering and diffraction have proved to be the largest components of differences between the results of satellite TSI results so far.

The usefulness of the laboratory cryo-radiometer calibration approach is clear from the experience of the ACRIM-SAT/ACRIM3 instrumentation described here. The results of the ACRIM3 and TIM experiments, both calibrated at the LASP/TRF after launch using surrogate flight backup instrumentation, agree much more closely than with their original calibrations—within the uncertainty of the technique (~500 ppm). A remaining challenge in this or any calibration approach is to verify the in-flight reproduction of the preflight calibration and that should be the focus of continuing research.

The calibration of the SI scale of the ACRIM3 instrumentation was found to be within the ~500 ppm of the TRF test uncertainty. The Scattering and diffraction net effect was found to increase TSI observations by 5025 ppm.

The TRF derived update to ACRIM3 results was therefore -5025 ppm and no correction was made for SI scale.

An algorithm update for the temperature dependent behavior of the ACRIM3 ADC was made based on the experience of more than a decade in flight. This update removed a spurious annual signal of ~ 300 ppm amplitude in the results, caused by the variation of spacecraft temperature between aphelion and perihelion. Another algorithm update optimized the parsing of shutter closed and open data which reduced the uncertainty of the results by minimizing the time between reference and solar observations. The net effect of these updates and the TRF scattering and diffraction corrections was to lower the average ACRIM3 results to within less than ± 200 ppm of the average TIM TSI values.

Detailed agreement of short term variations was found among the three sets of satellite TSI experimental results covering the last decade: the updated ACRIMSAT/ACRIM3, the SORCE/TIM and the SOHO/VIRGO. On a percentage variation basis the close agreement between these results in early 2003 (~ 50 ppm) was followed by a steady upward trend of TIM results, relative to ACRIM3 and VIRGO, reaching ~ 500 ppm by mid-2013. This divergence would appear to be a flaw in the TIM results since ACRIM3 and VIRGO continue to agree over the period to within ~ 50 ppm on average. The cause could be overcorrection of TIM sensor degradation or some other yet to be discovered factor. Since the uncertainty of self-calibration degradation for the ACRIM3 sensors is < 5 ppm/year during this period the divergence is significant and must be resolved to provide a long term TSI database with sufficient traceability for climate and solar physics research.

The composite TSI time series from late 1978 through mid-2013, compiled by relating adjacent overlapping TSI experimental results at their mutual levels of precision, is the most valuable use of the satellite data for climate and solar physics research. Two time series constructed using different sets of available data and approaches, the ACRIM and PMOD TSI composites, find significantly different trend results.

The ACRIM TSI composite uses results from ERB, ACRIM 1, ACRIM2 and ACRIM3 published by the science teams and the ERB results to connect the ACRIM1 and ACRIM2 across the ACRIM Gap (1989.5–1991.75). A key finding is an upward trend in TSI during the last decades of the 20th century (solar cycles 21–23) of $+0.037$ %/decade that is significant relative to the uncertainty of the observations (< 0.005 %/decade).

The PMOD TSI composite uses ERB, ACRIM1, ACRIM2 and VIRGO results to cover the 35 years of the satellite database. The PMOD modifies some ERB and ACRIM results to conform them to the predictions of TSI proxy models and chooses the scale of the ERBS/ERBE results to bridge the ACRIM Gap. The PMOD does not find the

ACRIM upward trend during solar cycles 21–23 but instead a marginally significant 0.008 %/decade downward trend.

The difference in TSI trending between the ACRIM and PMOD composites has been shown to be caused by the choice between the ERB and ERBE, respectively, to bridge the ACRIM Gap (Scafetta and Willson 2014). The resolution of the correct ACRIM Gap choice and TSI trend, the subject of much debate for two decades, now appears to be resolved. A new TSI proxy, compiled from the Kitt Peak National Solar Observatory records of solar magnetic field strength, has been used to show that the ACRIM TSI composite trend of 0.037 %/decade is the most likely correct interpretation of available TSI results. The ERBE results during the ACRIM Gap and therefore the PMOD TSI composite trend during solar cycles 21–23 are not supported by the solar magnetic field strength proxy. This is considered to be a definitive result since the solar magnetic field strength is a much more TSI-specific proxy than the Mg II and Ca II proxies utilized by others that are more specific for solar chromospheric ultra-violet radiation.

The purpose of precise TSI time series on climate time scales is to enable determination of the relative significance of TSI variability and other climate forcings. The TSI upward trend in the ACRIM composite during the last two decades of the 20th century is consistent with a larger role in forcing the global climate warming in that period than predicted by climate models. Ongoing investigations of climate change and its forcings cannot ignore the fact that historical records show that on decadal and longer time scales global climate trends always correlate with the solar magnetic activity level and TSI but have anti-correlated with the the CO_2 content of the atmosphere on a number of occasions.

Open Access This article is distributed under the terms of the Creative Commons Attribution License which permits any use, distribution, and reproduction in any medium, provided the original author(s) and the source are credited.

References

- Butler, J., et al.: Sources of differences in on-orbital total solar irradiance measurements and description of a proposed laboratory intercomparison. *J. Res. Natl. Inst. Stand. Technol.* **113**, 187–203 (2008)
- Datla, R.U., Stock, K., Parr, A.C., Hoyt, C.C., Miller, P.J., Foukal, P.V.: Characterization of an absolute cryogenic radiometer as a standard detector for radiant-power measurements. *Appl Opt.* **31**(34), 7219–7225 (1992). doi:[10.1364/AO.31.007219](https://doi.org/10.1364/AO.31.007219)
- Eddy, J.A.: Climate and the changing sun. *Clim. Change* **1**, 173–190 (1977)
- Frohlich, C.: VIRGO radiometry. In: International Space Science Institute Proceedings (2013)
- Frohlich, C., Lean, J.: The Sun's total irradiance: cycles and trends in the past two decades and associated climate change uncertainties. *Geophys. Res. Lett.* **25**, 4377–4380 (1998)

- Frohlich, C., Lean, J.: Solar radiative output and its variability: evidence and mechanisms. *Astron. Astrophys. Rev.* (2004). doi:[10.1007/s00159-004-0024-1](https://doi.org/10.1007/s00159-004-0024-1)
- Frohlich, C., Crommelynck, D., Wehrli, C., Anklin, M., Dewitte, S., Fichot, A., Finsterle, W., Jiménez, A., Chevalier, A., Roth, H.J.: In-flight performances of VIRGO solar irradiance instruments on SOHO. *Sol. Phys.* **162**, 101–128 (1997)
- Hickey, J.R., et al.: Total solar irradiance measurements by ERB/Nimbus-7—A review of nine years. *Space Sci. Rev.* **48**(3–4), 321–342 (1988). doi:[10.1007/BF00226011](https://doi.org/10.1007/BF00226011)
- Houston, J.M., Rice, J.P.: NIST reference cryogenic radiometer designed for versatile performance. *Metrologia* **43**(2), S31–S35 (2006). doi:[10.1088/0026-1394/43/2/S07](https://doi.org/10.1088/0026-1394/43/2/S07)
- Hoyt, D.V., et al.: The Nimbus 7 solar total irradiance: a new algorithm for its derivation. *J. Geophys. Res.* **97**(A1), 51–63 (1992)
- Kopp, G., Lean, J.L.: A new, lower value of total solar irradiance: Evidence and climate significance. *Geophys. Res. Lett.* **38**, L01706 (2011a). doi:[10.1029/2010GL045777](https://doi.org/10.1029/2010GL045777)
- Kopp, G., Lean, J.L.: Uncertainties spanning potential SORCE/TIM to JPSS/TIM Gap (Study A), National Research Council. In: Review of NOAA Working Group Report on Maintaining the Continuation of Long-Term Satellite Total Irradiance Observations. The National Academies Press, Washington (2011b)
- Kopp, G., Lean, J.L.: The solar climate data record: scientific assessment of strategies to mitigate an impending gap in total solar irradiance observations between the NASA SORCE and NOAA TSIS Missions (Study B), National Research Council. In: Review of NOAA Working Group Report on Maintaining the Continuation of Long-Term Satellite Total Irradiance Observations. The National Academies Press, Washington (2013)
- Kopp, G., Heuerman, K., Lawrence, G.: The Total Irradiance Monitor (TIM): instrument calibration. *Sol. Phys.* **230**, 111–127 (2005b)
- Kopp, G., Lawrence, G., Rottman, G.: The Total Irradiance Monitor (TIM): science results. *Sol. Phys.* **230**(1), 129–140 (2005a)
- Kopp, G., Heuerman, K., Harber, D., Drake, V.: The TSI radiometer facility—absolute calibrations for total solar irradiance instruments. *Proc. SPIE* **6677**, 667709 (2007). doi:[10.1117/12.734553](https://doi.org/10.1117/12.734553)
- Kopp, G., Fehlmann, A., Finsterle, W., Harber, D., Heuerman, K., Willson, R.: Total solar irradiance data record accuracy and consistency improvements. *Metrologia* **49**, S29 (2012). doi:[10.1088/0026-1394/49/2/S29](https://doi.org/10.1088/0026-1394/49/2/S29)
- Krivova, N.A., Balmaceda, L., Solanki, S.K.: Reconstruction of solar total irradiance since 1700 from the surface magnetic flux. *Astron. Astrophys.* **467**, 335–346 (2007)
- Lean, J., Beer, J., Bradley, R.: Reconstruction of solar irradiance since 1610: implications for climate change. *Geophys. Res. Lett.* **22**, 3195–3198 (1995)
- Lee, R.B. III, Gibson, M.A., Wilson, R.S., Thomas, S.: Long-term total solar irradiance variability during sunspot cycle 22. *J. Geophys. Res.: Space Phys.* **100**(A2), 1667–1675 (1995). doi:[10.1029/94JA02897](https://doi.org/10.1029/94JA02897)
- Martin, J.E., Fox, N.P., Key, P.J.: A cryogenic radiometer for absolute radiometric measurements. *Metrologia* **21**, 147 (1985). doi:[10.1088/0026-1394/21/3/007](https://doi.org/10.1088/0026-1394/21/3/007)
- Meftah, M., Dewitte, S., Irbah, A., Chevalier, A., Conscience, C., Crommelynck, D., Janssen, E., Mekaoui, S.: SOVAP/PICARD, a spaceborne radiometer to measure the Total Solar Irradiance. *Solar Phys.* (2013) doi:[10.1007/s11207-013-0443-0](https://doi.org/10.1007/s11207-013-0443-0)
- Morrill, J., Socker, D., Thernisien, A., McMullin, D., Shirley, E., Hanssen, L., Zeng, J., Lorentz, S.: Final Report—NRL Support of ACRIMSAT Mission Extension (NASA Grant NNN10AO22), Naval Research Laboratory, March 1, 2013
- Scafetta, N., West, B.J.: Phenomenological reconstructions of the solar signature in the Northern Hemisphere surface temperature records since 1600. *J. Geophys. Res.* **112**, D24S03 (2007). doi:[10.1029/2007JD008437](https://doi.org/10.1029/2007JD008437)
- Scafetta, N., Willson, R.C.: ACRIM Gap and Total Solar Irradiance (TSI) trend issue resolved using a surface magnetic flux TSI proxy model. *Geophys. Res. Lett.* **36**, L05701 (2009). doi:[10.1029/2008GL036307](https://doi.org/10.1029/2008GL036307)
- Scafetta, N., Willson, R.C.: Multiscale comparative spectral analysis of satellite total solar irradiance measurements from 2003 to 2013 reveals a planetary modulation of solar activity and its non-linear dependence on the 11 yr solar cycle (2013). doi:[10.5194/prp-1-1-2013](https://doi.org/10.5194/prp-1-1-2013)
- Scafetta, N., Willson, R.C.: Empirical evidences for a planetary modulation of total solar irradiance and the TSI signature of the 1.09-year Earth-Jupiter conjunction cycle. *Astrophys. Space Sci.* (2013). doi:[10.1007/s10509-013-1558-3](https://doi.org/10.1007/s10509-013-1558-3)
- Scafetta, N., Willson, R.C.: ACRIM total solar irradiance satellite composite validation versus TSI proxy models. *Astrophys. Space Sci.* (2014). doi:[10.1007/s10509-013-1775-9](https://doi.org/10.1007/s10509-013-1775-9)
- Schmutz, W., Fehlmann, A., Finsterle, W., Kopp, G., Thuillier, G.: Total solar irradiance measurements with PREMOS/PICARD. *AIP Conf. Proc.* **1531**, 624 (2013). doi:[10.1063/1.4804847](https://doi.org/10.1063/1.4804847)
- Wenzler, T., Solanki, S.K., Krivova, N.A., Frohlich, C.: Reconstruction of solar irradiance variations in cycles 21–23 based on surface magnetic fields. *Astron. Astrophys.* **460**, 583–595 (2006)
- Wenzler, T., Solanki, S.K., Krivova, N.A.: Reconstructed and measured total solar irradiance: Is there a secular trend between 1978 and 2003? *Geophys. Res. Lett.* **36**, L11102 (2009). doi:[10.1029/2009GL037519](https://doi.org/10.1029/2009GL037519)
- Willson, R.C.: Radiometer Comparison Tests. JPL Technical Memorandum 33-371, Jet Propulsion Laboratory, Pasadena, CA, USA (1967)
- Willson, R.C.: Active cavity radiometric scale, international pyrheliometric scale, and solar constant. *J. Geophys. Res.* **76**(19), 4325–4340 (1971). doi:[10.1029/JA076i019p04325](https://doi.org/10.1029/JA076i019p04325)
- Willson, R.C.: Active cavity radiometer. *Appl. Opt.* **12**(4), 810–817 (1973). doi:[10.1364/AO.12.000810](https://doi.org/10.1364/AO.12.000810)
- Willson, R.C.: Accurate solar ‘constant’ determinations by cavity pyrheliometers. *J. Geophys. Res.* **83**(C8), 4003–4007 (1978). doi:[10.1029/JC083iC08p04003](https://doi.org/10.1029/JC083iC08p04003)
- Willson, R.C.: Active cavity radiometer type IV. *Appl. Opt.* **18**(2), 179–188 (1979). doi:[10.1364/AO.18.000179](https://doi.org/10.1364/AO.18.000179)
- Willson, R.C.: Active cavity radiometer type V. *J. Appl. Opt.* **19**(19), 3256–3257 (1980). doi:[10.1364/AO.19.003256](https://doi.org/10.1364/AO.19.003256)
- Willson, R.C.: Measurements of solar total irradiance and its variability. *Space Sci. Rev.* **38**(3–4), 203–242 (1984). doi:[10.1007/BF00176830](https://doi.org/10.1007/BF00176830)
- Willson, R.C.: Total solar irradiance trend during solar cycles 21 and 22. *Science* **277**(5334), 1963–1965 (1997). doi:[10.1126/science.277.5334.1963](https://doi.org/10.1126/science.277.5334.1963)
- Willson, R.C.: ACRIMSAT/ACRIM3 Algorithm Theoretical Basis Document (1999)
- Willson, R.C.: The ACRIMSAT/ACRIM3 Experiment—Extending the Precision, Long-Term Total Solar Irradiance Climate Database, NASA, The Earth Observer, May–June, 2001
- Willson, R.C.: LASP_TRF diagnostic test results for the ACRIM3 experiment and their implications for the multi-decadal TSI database. In: SORCE Science Team Meeting Proceedings, Sedona, AZ, Sep. 13–16, 2011
- Willson, R.C., Hudson, H.S.: The Sun’s luminosity over a complete solar cycle. *Nature* **351**, 42–44 (1991). doi:[10.1038/351042a0](https://doi.org/10.1038/351042a0)
- Willson, R.C., Mordvinov, A.V.: Secular total solar irradiance trend during solar cycles 21–23. *Geophys. Res. Lett.* **30**, 1199 (2003). doi:[10.1029/2002GL016038](https://doi.org/10.1029/2002GL016038)
- Willson, R.C., Gulkis, S., Janssen, M., Hudson, H.S., Chapman, G.A.: Observations of solar irradiance variability. *Science* **211**, 700 (1981). doi:[10.1126/science.211.4483.700](https://doi.org/10.1126/science.211.4483.700)
- Willson, R.C., Hudson, H.S., Frohlich, C., Brusa, R.W.: Long term downward trend in total solar irradiance. *Science* **234**, 1114 (1986)